

Electronic Supplementary Information

Vapor Selenization Produced Bi₂Se₃ Nanoparticles in Carbon Fibers 3D Network as Binder-Free Anode for Flexible Lithium-Ion Batteries

Hong-Qing Qu,^{†a} Hong Yin,^{†a,b,c} Ya-Long Wang,^a Cheng Fan,^a Kwun Nam Hui,^b Chong Li*^a and Ming-Qiang Zhu^a

^aWuhan National Laboratory for Optoelectronics (WNLO), School of Optics and Electronic Information, Huazhong University of Science and Technology, Wuhan 430074, China

^bInstitute of Applied Physics and Materials Engineering, University of Macau, Avenidada Universidade, Taipa, Macau, China

^cDepartment of Bioengineering, University of California, Los Angeles, Los Angeles, CA 90095, USA

*Corresponding Authors

E-mail: chongli@hust.edu.cn

[†]These authors contributed equally to the work.

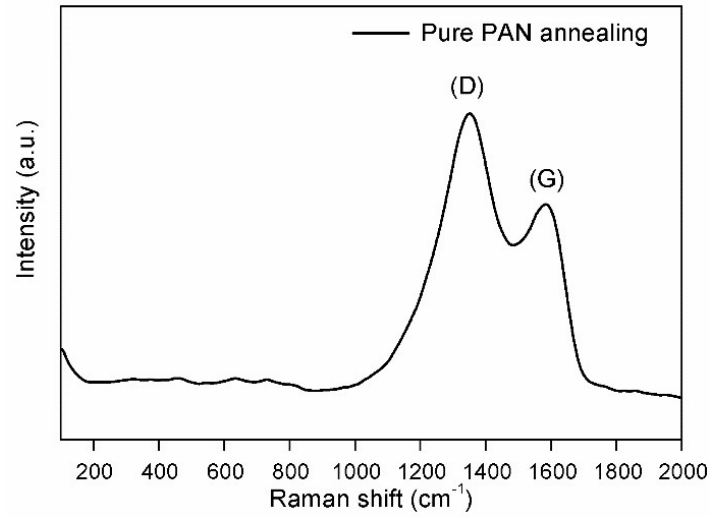


Fig. S1. Raman spectra of the pure PAN after annealing at 700 °C for 6 h.

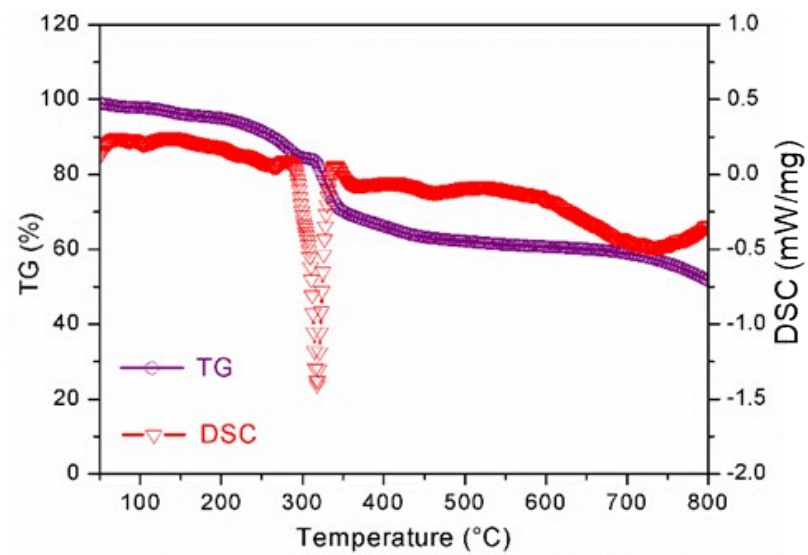
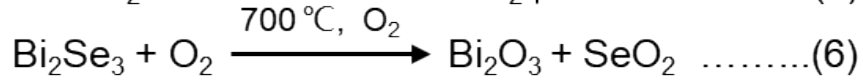
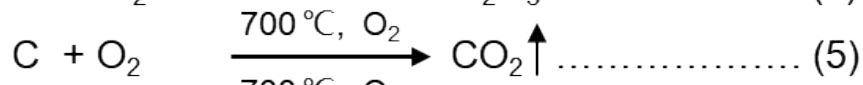
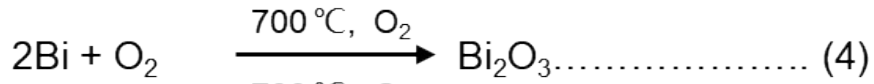


Fig. S2. TGA-DSC curves of the BiCl₃/PAN.

Depiction S1



The content of Bi nanoparticles in Bi/CNFs can be calculated by calculation combining equation (4) and (5). In the same way, the content of Bi₂Se₃ nanoparticles in Bi₂Se₃/CNFs can be calculated by calculation combining equation (6).

$$\text{Bi (\%)} = \frac{\text{Final weight of Bi}_2\text{O}_3}{\text{Initial weight of Bi/CNFs}} \times \frac{\text{Molecular weight of Bi} \times 2}{\text{Molecular weight of Bi}_2\text{O}_3} \times 100\%$$

$$\text{Bi}_2\text{Se}_3 (\%) = \frac{\text{Final weight of Bi}_2\text{O}_3}{\text{Initial weight of Bi}_2\text{Se}_3/\text{CNFs}} \times \frac{\text{Molecular weight of Bi}_2\text{Se}_3}{\text{Molecular weight of Bi}_2\text{O}_3} \times 100\%$$

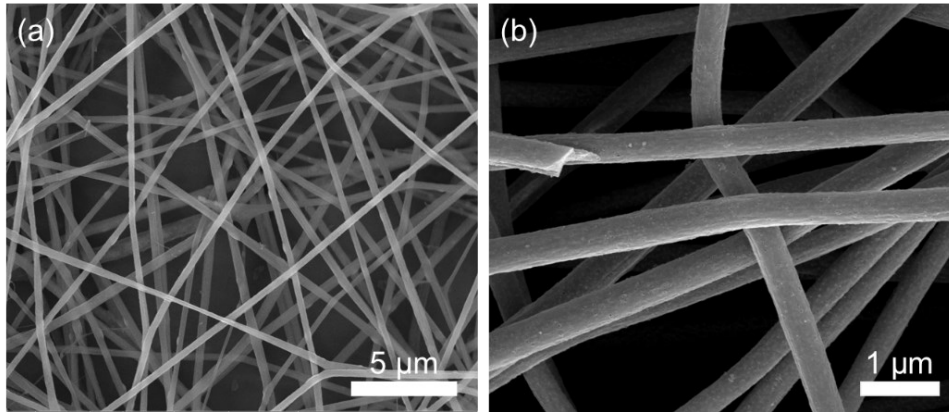


Fig. S3. SEM images of (a) BiCl₃/PAN and (b) Bi/CNFs.

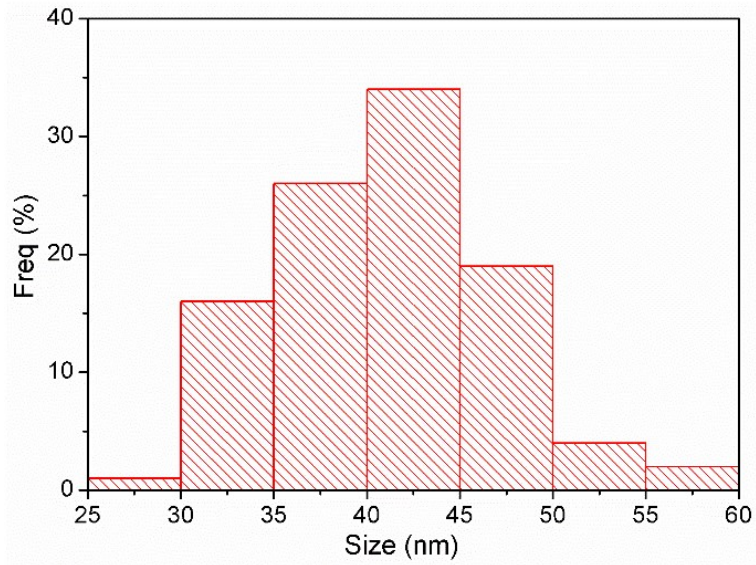


Fig. S4. The particle size distribution of Bi₂Se₃ nanoparticles.

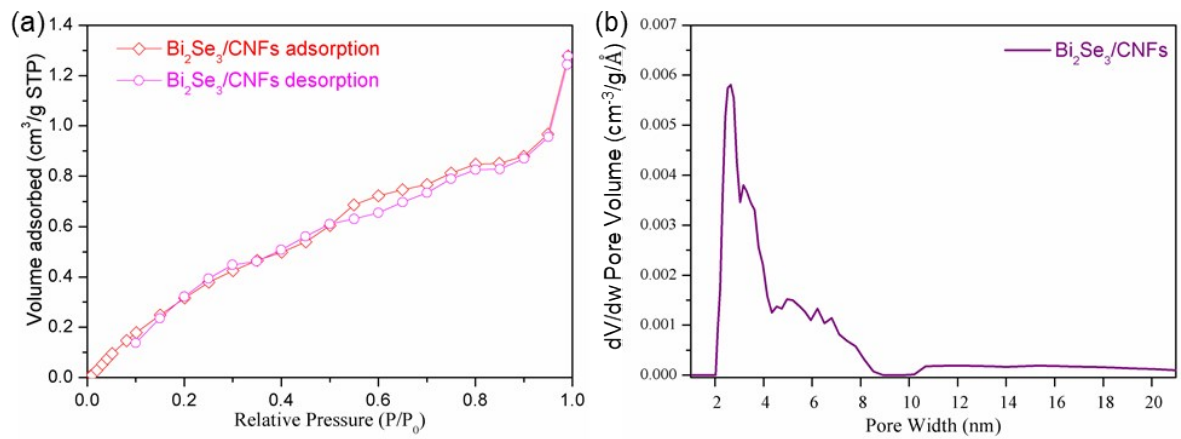


Fig. S5. (a) N₂ adsorption-desorption isotherms and (b) the pore size distribution of the Bi₂Se₃/CNFs.

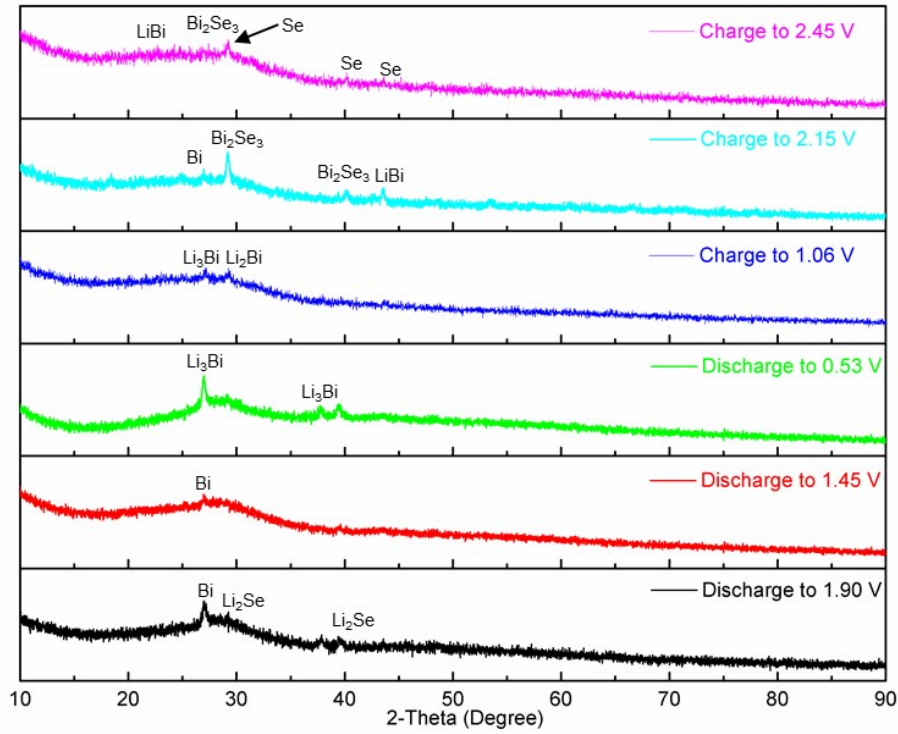


Fig. S6. The ex-situ XRD patterns of a new battery discharged and charged to different voltage platforms in the third cycle with Cu K α 1 (40 kV, 40 mA, $10^\circ < 2\theta < 90^\circ$)

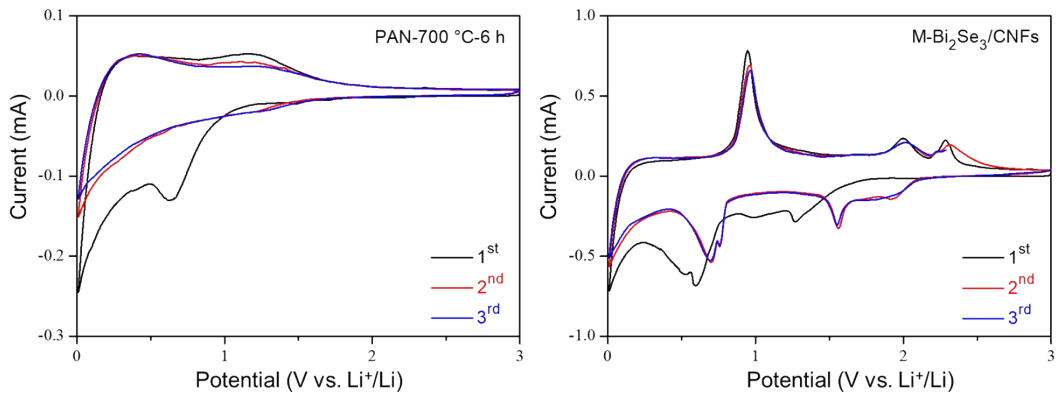


Fig. S7. CV curves of the (a) PAN was annealed at 700 °C for 6 h and (b) M-Bi₂Se₃/CNFs electrode from 3.0 V to 0.01 V vs. Li⁺/Li at a scan rate of 0.1 mV s⁻¹.

Table S1. The specific capacity of our work for LIBs vs. previous works.

Sample	Current	Cycles	Capacity vs Li ⁺ (mAh g ⁻¹)	Ref.
Bi ₂ Se ₃ rectangular nanosheets	50 mA g ⁻¹	50	34	[1]
Bi ₂ Se ₃ stacking nanosheets	50 mA g ⁻¹	50	45	[2]
In-doped Bi ₂ Se ₃	50 mA g ⁻¹	50	160.3	[3]
Hierarchical Bi ₂ Se ₃ microrods	50 mA g ⁻¹	50	36	[4]
Bi ₂ Se ₃ nanosheets	50 mA g ⁻¹	50	66.1	[5]
Bi ₂ Se ₃ /Graphene	50 mA g ⁻¹	100	203.6	[6]
S-doped Bi ₂ Se ₃	200 mA g ⁻¹	100	109.4	[7]
CNTs@C@Bi ₂ Se ₃	100 mA g ⁻¹	100	431	[8]
	2 A g ⁻¹	100	222	
Bi ₂ Se ₃ @NC	100 mA g ⁻¹	50	410.6	[9]
	500 mA g ⁻¹	400	335.8	
Flexible Bi ₂ Se ₃ /CNFs	100 mA g ⁻¹	100	443	Our work
	400 mA g ⁻¹	100	308	
	2 A g ⁻¹	100	189	
	16 A g ⁻¹	100	103	

Depiction S2

Synthesis of Bi_2Se_3 nanosheets: 0.75 g $\text{Bi}(\text{NO}_3)_3 \cdot 5\text{H}_2\text{O}$, 1.0 g of SeO_2 and 1.0 g of glucose were dissolved in an appropriate amount of deionized water and continuously stirred to obtain the mixed solution A. After continuous stirring to completely dissolve the powders, 20 mL ethanolamine was added to solution A under magnetic stirring, and mixed solution B was obtained after uniform stirring. Transfer the mixed solution B to a 60 mL Teflon stainless steel reactor and add deionized water until it reaches 80% of the total volume. The autoclave reacts for 30 h at 180 °C, and after natural cooling, the filtered products are washed several times with distilled water and anhydrous ethanol, and then dried for 6 hours in a vacuum drying oven at 60 °C.¹⁰

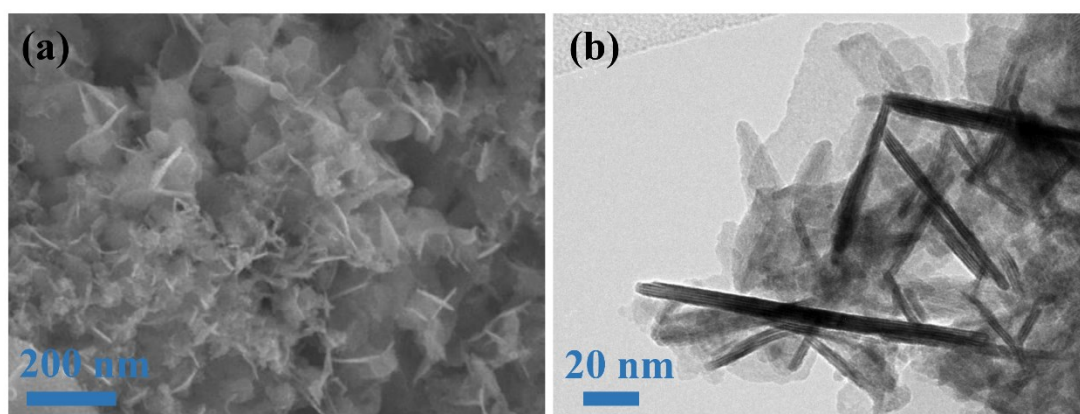


Fig. S8. (a) SEM image of Bi_2Se_3 nanosheets. (b) TEM image of Bi_2Se_3 nanosheets.

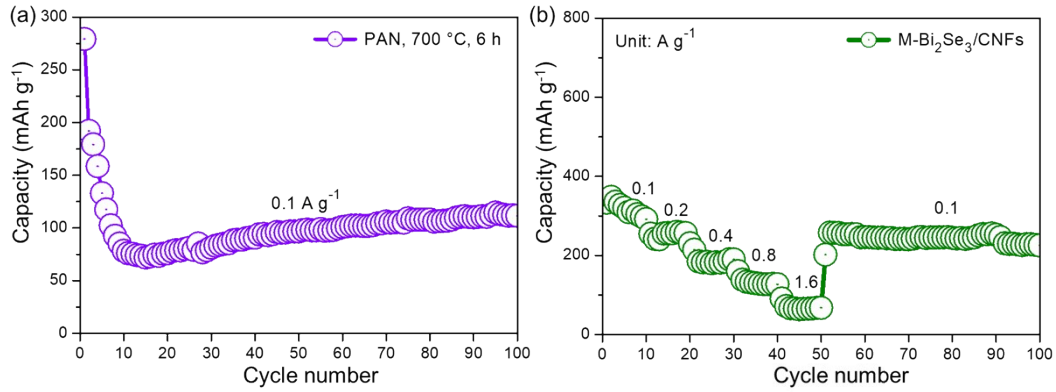


Fig. S9. (a) The specific discharge capacity of pure carbon nanofibers at a cycling rate of 0.1 A g^{-1} . (b) Rate capability of the $\text{M-Bi}_2\text{Se}_3/\text{CNFs}$ electrode at various current rates from 0.1 A g^{-1} to 1.6 A g^{-1} .

Depiction S3

The diffusion coefficient of lithium ions and electric conductivity in open circuit state are calculated by the following formula:

$$D = R^2 T^2 / 2 A^2 n^4 F^4 C^2 \sigma^2 \dots\dots (1) \quad Z_{\text{Re}} = K + \sigma \omega^{-1/2} \dots\dots (2)$$

where D is the diffusion coefficient ($\text{cm}^2 \text{ s}^{-1}$), R is the gas constant ($8.31 \text{ J mol}^{-1} \text{ K}^{-1}$), T is the absolute temperature (298 K), A is the surface area of the cathode (0.5 cm^2), n is the number of electrons transferred in the half-reaction for the redox couple, F is the Faraday constant (96485 C mol^{-1}), C is the molar concentration of Li-ions in $\text{Bi}_2\text{Se}_3/\text{CNFs}$ electrode, K is a constant, ω is frequency, and σ is the Warburg factor which corresponds to the slope of the curve shown in **Fig. 6b**.^{11,12}

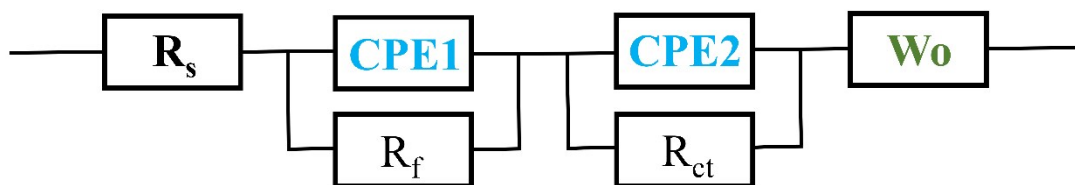


Fig. S10. Equivalent circuit diagram of Electrochemical Impedance Spectroscopy

Table S2. The linear correlation fitting results of Bi₂Se₃/CNFs, M-Bi₂Se₃/CNFs and Bi₂Se₃ nanosheets electrodes, respectively.

Sample	Bi ₂ Se ₃ /CNFs	M-Bi ₂ Se ₃ /CNFs	Bi ₂ Se ₃ Nanosheets
Intercept	67.6	111.2	84.8
Slope	17.6	60.3	250.3

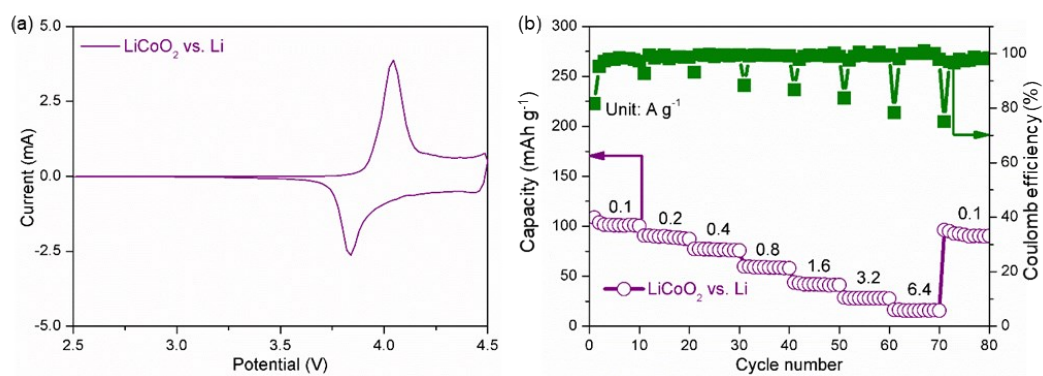


Fig. S11. (a) The CV curve with a sweep speed of 0.1 mV s⁻¹ and (b) rate performance of LiCoO₂ cathode with current density from 0.1 A g⁻¹ to 6.4 A g⁻¹.

References:

1. Ali Z, Cao C, Li J, Wang Y, Cao T, M. Tanveer, Muhammad Tahir, Faryal Idrees, Faheem K. Butt, Effect of synthesis technique on electrochemical performance of bismuth selenide, *J. Power Sources*, 2013, **229**, 216-222.
2. Xu H, Chen G, Jin R, Chen D, Wang Y, and Jian Pei, Green synthesis of Bi_2Se_3 hierarchical nanostructure and its electrochemical properties, *Rsc Adv.*, 2014, **4**, 8922-8929.
3. G. Han, Z. Chen, D. Ye, L. Yang, L. Wang, J. Drennan and J. Zou, In-doped Bi_2Se_3 hierarchical nanostructures as anode materials for Li-ion batteries, *J. Mater. Chem. A*, 2014, **2**, 7109-7116.
4. Xu H, Chen G, Jin R, Pei J, Wang Y, and Chen D, Hierarchical Bi_2Se_3 microrods: microwave-assisted synthesis, growth mechanism, and their related properties, *CrstyEngComm*, 2013, **15**, 1618-1625.
5. R. Jin, J. Liu, Y. Xu, G. Li, G. Chen and L. Yang, Hierarchical $\text{Bi}_2\text{Se}_{3-x}\text{S}_x$ microarchitectures assembled from ultrathin polycrystalline nanosheets: solvothermal synthesis and good electrochemical performance, *J Mater. Chem. A.*, 2013 **1**, 10942-10950.
6. X. Chen, H. Tang, Z. Huang, J. Zhou, X. Ren, K. Huang, X. Qi and J. Zhong, Flexible Bismuth Selenide/Graphene composite paper for lithium-ion batteries, *Ceram. Int.*, 2017, **43**, 1437-1442.
7. F. Mao, J. Guo, S. Zhang, F. Yang, Q. Sun, J. Ma and Z. Li, Solvothermal synthesis and electrochemical properties of S-doped Bi_2Se_3 hierarchical microstructure assembled by stacked nanosheets, *Rsc Adv.*, 2016, **6**, 38228-38232.
8. R. Jin, M. Sun, G. Li, CNTs@C@ Bi_2Se_3 composite as an improved-performance anode for lithium ion batteries, *Ceram. Int.*, 2017, **43**, 17093-17099.
9. Z. Li, H. Pan, W. Wei, A. Dong, K. Zhang, H. Lv and X. He, Bismuth metal-organic frameworks derived bismuth selenide nanosheets/nitrogen-doped carbon hybrids as anodes for Li-ion batteries with improved cyclic performance, *Ceram. Int.*, 2019, **45**, 11861-11867.
10. H. Fan, S. Zhang, P. Ju, H. Su and S. Ai, Flower-like Bi_2Se_3 nanostructures: Synthesis and their application for the direct electrochemistry of hemoglobin and H_2O_2 detection, *Electrochim. Acta*, 2012, **64**, 171-176.
11. H. Yin, H. Q. Qu, Z. Liu, R. Z. Jiang, C. Li and M. Q. Zhu, Long cycle life and high rate capability of three dimensional CoSe_2 grain-attached carbon nanofibers for flexible sodium-ion batteries, *Nano Energy*, 2019, **58**, 715-723.

12. H. Yin, M. Cao, X. Yu, H. Zhao, Y. Shen, C. Li and M. Zhu, Self-standing Bi₂O₃ nanoparticles/carbon nanofiber hybrid films as a binder-free anode for flexible sodium-ion batteries, *Mater. Chem. Front.*, 2017, **1**, 1615-1621.